Water Science & Technology

IWA PUBLISHING

Water Science & Technology Vol 84 No 9, 2278 doi: 10.2166/wst.2021.421

Improvement of stability and reduction of energy consumption for Ti-based MnO_x electrode by Ce and carbon black co-incorporation in electrochemical degradation of ammonia nitrogen

Jiao Zhao [a,*], Xuelu Xu[b], Zehui Liu[a], Xiaodan Bai[a], Yan Yang [a], Xiaoyi Li[a], Yin Wang[a], Weifeng Liu [a] and Yimin Zhu[a]

[a] Collaborative Innovation Center for Vessel Pollution Monitoring and Control, Dalian Maritime University, Dalian 116026, China
[b] College of Architecture and Civil Engineering, Shenyang University of Technology, Shenyang 110870, China
*Corresponding author. E-mail: zhaojiao@dlmu.edu.cn
Jiao Zhao and Xuelu Xu contributed equally to this work.

JZ, 0000-0003-0891-0909; YY, 0000-0002-9328-6815; WL, 0000-0003-3710-8173

ABSTRACT

Ti-based electrode coated with MnO_x catalytic layer has presented superior electrochemical activity for degradation of organic pollution in wastewater, however, the industrial application of Ti-based MnO_x electrode is limited by the poor stability of the electrode. In this study, the novel Ti-based MnO_x electrodes co-incorporated with rare earth (Ce) and conductive carbon black (C) were prepared by spraying-calcination method. The Ti/Ce:MnO_x-C electrode, with uniform and integrated surface and enhanced Mn(IV) content by C and Ce co-incorporation, could completely remove ammonia nitrogen (NH_4^+-N) with N_2 as the main product. The cell potential and energy consumption of Ti/Ce:MnO_x-C electrode during the electrochemical process was significantly reduced compared with Ti/MnO_x electrode, which mainly originated from the enhanced electrochemical activity and reduced charge transfer resistance by Ce and C co-incorporation. The accelerated lifetime tests in sulfuric acid showed that the actual service lifetime of Ti/Ce:MnO_x-C was ca. 25 times that of Ti/MnO_x, which demonstrated the significantly promoted stability of MnO_x-based electrode by Ce and C co-incorporation.

Key words: ammonia nitrogen (NH_4^+-N), electrochemical oxidation, MnOx, Ti-based electrodes, wastewater remediation

HIGHLIGHTS

- The Ti-based MnOx electrodes co-incorporated with Ce and C were prepared and served as electrocatalysts to remove ammonia nitrogen.
- The cell potential and energy consumption of Ti/Ce:MnOx-C was reduced by 35% compared with Ti/MnOx, originating from the enhanced activity and reduced resistance.
- The service lifetime of Ti/Ce:MnOx-C was improved by 25 times compared with Ti/MnOx, demonstrating the promoted stability.

GRAPHICAL ABSTRACT

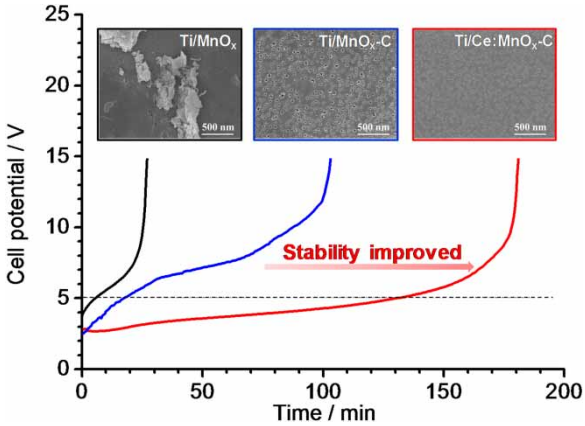

INTRODUCTION

Well-developed methods, classified as physical technology, chemical technology and biological technology, have been applied to wastewater treatment. The physical technologies include coagulation/flocculation (Mamelkina *et al.* 2020), separation membrane (Tavangar *et al.* 2020) and adsorption (Bacelo *et al.* 2020; Choudhary *et al.* 2020; Imran *et al.* 2021). The biological treatments have been studied, including anaerobic process, activated sludge process and so on (Gopalakrishnan *et al.* 2019; Wu *et al.* 2021). The chemical technology, such as ozonation and oxidation with catalysts (Silva *et al.* 2019; Liu *et al.* 2021), as well as advanced oxidation processes (AOPs), has been widely used in wastewater treatment due to its effectiveness. Electrochemical oxidation (EO) technology, as one of the AOPs, has attracted considerable attention for wastewater remediation, because it could completely mineralize refractory organic pollutants and present several characteristics of environmental significance without generating secondary pollutants, such as mild operation conditions, strong adaptability, simple and reliable equipment, and so on (Brillas & Martínez-Huitle 2015; Dominguez *et al.* 2018; Garcia-Segura *et al.* 2018). In EO remediation of wastewater, anode materials play particularly important roles, which could determine the degradation efficiency and service lifetime of the electrodes. Dimensionally stable anode, an electrode prepared by active metal oxides coated on the titanium substrate, has been successfully employed to degrade various refractory pollutants, and shows potential to overcome the poor stability of traditional graphite electrodes (Zhu *et al.* 2019) and high cost of noble metal electrodes (Tavares *et al.* 2012). A variety of electrodes, such as Ti/PbO_2 (Polcaro *et al.* 1999; Bian *et al.* 2019), Ti/SnO_2 (Martínez-Huitle *et al.* 2008), Ti/RuO_2 (Yue *et al.* 2017), and Ti/IrO_2 (Baddouh *et al.* 2020) have been investigated as anode for the EO remediation of wastewater because they are effective in oxidizing pollutants with high oxygen overpotentials. However, the high cost and inefficient performance for high-chloride content wastewater limits their use (Kaur *et al.* 2017). And the large-scale application is also limited due to leakage of metal cations during preparation process and by electrochemical corrosion, which may cause secondary pollution (Li *et al.* 2016). Therefore, it is essential to develop electrodes with superior catalytic activity, high stability, low cost and mild toxicity.

Ti/MnO_x anodes are regarded as promising candidates in EO remediation of wastewater because of the low cost and toxicity, ease of preparation, and high electro-catalytic activity. Yang *et al.* reported porous Ti/MnO_x anode for degradation of phenol in electro-catalytic membrane reactor, and the phenol removal efficiency was 93%, with chemical oxygen demand (COD) and total organic carbon (TOC) removal efficiency of 79 and 68%, respectively (Yang *et al.* 2018). Massa's reports suggested that MnO_x could promote the direct and indirect oxidation of phenol in EO remediation of wastewater (Massa *et al.* 2018). Hui *et al.* prepared porous Ti/MnO_x anode for degradation of highly concentrated phenol in wastewater, and the phenol removal efficiency was 73% in fixed bed electro-catalytic reactor (Hui *et al.* 2019). Our previous results also demonstrated the superior activity of Ti/MnO_x anodes in electrochemical degradation of Acid Red B, a typical azo dye in textile wastewater (Xu *et al.* 2019). Even though MnO_x-based electrodes present superior electro-catalytic activity for removal of organic pollution, and have been widely studied in water oxidation, lithium-ion batteries and supercapacitors, the commercial application of Ti/MnO_x electrode is still hindered by the short lifetime (Jiang & Kucernak 2002; Martínez-Huitle *et al.* 2008; Wiechen *et al.* 2012; Xiang *et al.* 2015; Wang *et al.* 2018).

Ammonia nitrogen (NH_4^+-N) in wastewater is an increasing problem, which can promote eutrophication and is toxic to aquatic organisms. Even though most of the NH_4^+-N can be removed by biological method in practical application (Del Moro *et al.* 2016), low concentration of NH_4^+-N is very difficult to remove, and the concentration of NH_4^+-N needs to be in accordance with a specified detection limit. Previous studies have demonstrated that NH_4^+-N could be decomposed to N_2 mainly by electrochemical degradation process (Zöllig *et al.* 2015). To the best of our knowledge and according to the literature review, there is no report on the study of Ti/MnO_x anodes in electrochemical degradation of NH_4^+-N from an aqueous solution. In the present work, we introduced conductive carbon black (C) and Ce into the MnO_x catalytic layer to fabricate a Ti/Ce:MnO_x-C electrode. The surface characteristics and electrochemical properties of Ti/Ce:MnO_x-C electrode were studied, and the degradation efficiency, cell potential, energy consumption, and stability of Ti/Ce:MnO_x-C electrode were compared with MnO_x/Ti in electrochemical degradation of NH_4^+-N. Studies showed that Ti/Ce:MnO_x-C electrode presented significantly improved lifetime and reduced energy consumption with the co-incorporation of C and Ce.

EXPERIMENTAL

Materials and reagents

Titanium plate was purchased from Suzhou Shuertai Industrial Technology Co., Ltd (Suzhou, China). Isopropanol and oxalic acid were purchased from Tianjin Damao Chemical Reagent Factory (Tianjin, China). Conductive carbon black was purchased from Tianjin Yiborui Chemical Co. Ltd (Tianjin, China). Ammonia sulfate, manganese nitrate (50%), cerium nitrate hexahydrate, sulfuric acid, sodium hydroxide, sodium chloride and sodium sulfate were purchased from Sinopharm Group Chemical Reagent Co., Ltd (Shanghai, China). All chemical reagents employed were of analytical purity grade. Ultra-purified water with resistivity of 18.2 MΩ·cm was obtained from the Millipore-Q system for all of the solutions.

Electrode preparation

First, titanium plate was pretreated by polishing, caustic washing and acid etching. Then 5 mL of $Mn(NO_3)_2$ isopropanol solution (1 mmol) was sprayed onto the pretreated Ti substrate at pressure of 4 kPa by the spray gun (caliber: 0.2 mm). After that, the Ti plate was dried at 100 °C for 10 min and then thermally treated at 200 °C for 5 min. The above processes were repeated four times. Finally, the product was calcinated at 350 °C for 20 min to obtain Ti/MnO_x electrode. Ti/MnO_x-C electrode was prepared with a certain amount of conductive carbon black (C) added into the $Mn(NO_3)_2$ solution during the spraying process. The molar ratio of C/Mn was 14%. As for the Ti/Ce:MnO_x-C electrode, the spraying solution was a mixture of conductive carbon black (C), $Ce(NO_3)_2{\cdot}6H_2O$ and $Mn(NO_3)_2$ with C/Mn molar ratio of 14% and Ce/Mn molar ratio of 1%. The active area of the prepared electrodes was 4 cm^2.

Electrode characterization

The powder X-ray diffraction (XRD) data were collected on X'PERT PRO type X-ray diffraction (Netherlands Spectris) with CuKα radiation ($\lambda = 1.5418$ Å) over the 2θ range of 5° to 80° with scan speed of 5°/min at room temperature. The scanning electron microscopy (SEM) was undertaken by JSM-7500F cold field emission scanning electron microscope (Japan Electronics Co., Ltd) at accelerating voltage of 20 kV. The X-ray photoelectron spectroscopy (XPS) was performed using ESCALAB250 (American Thermo VG Co., Ltd) equipped with an Al Kα source.

Electrochemical experiment

Electrochemical experiments were performed in a conventional three-electrode cell system at CHI660E electrochemical workstation (Shanghai Chenhua Instrument Co., Ltd, China). The prepared electrodes were employed as working electrode with platinum electrode (20 mm × 30 mm × 0.1 mm) as the counter electrode, and Ag/AgCl/0.1 M KCl (Shanghai Ciyue Electronic Technology Co., Ltd, China) as the reference electrode. The cyclic voltammetry (CV) measurement was conducted in 0.1 mol/L sodium sulfate solution at scan rate of 50 mV/s with scan region from 0 to 2.5 V. The polarization curve (linear sweep voltammetry; LSV) was tested at scan rate of 10 mV/s in 0.1 mol/L sodium sulfate and 400 mg/L sodium chloride solution. The conductivity of the electrodes was tested by electrochemical impedance spectroscopy (EIS) with the frequency range from 1×10^5 to 1×10^{-2} Hz and the amplitude of 10 mV, which was conducted at open circuit potential. All of the electrodes were activated by cyclic voltammetry at 50 mV/s before the tests.

Electrode activity test

The electrochemical degradation of ammonia nitrogen, prepared by ammonia sulfate with concentration of 23 mg/L, was conducted in an electrochemical system with 0.1 mol/L sodium sulfate and 400 mg/L sodium chloride as supporting

electrolyte at pH 9.0. The prepared electrode and pure titanium plate served as anode and cathode, respectively, with the distance of 1 cm between them. Constant current was chosen by a direct current power supply (DC stabilized power supply, KPS-3005D, Zhaoxin Electronic Equipment Co., Ltd, China) over reaction time of 90 min. The simulated wastewater was electrochemically degraded at 20 mA/cm^2 with magnetic stirring at room temperature. The cell potentials were recorded by data recorder (34970A, Keithley Instruments, USA). The concentration of NH_4^+-N in the wastewater was analyzed on a DR3900 spectrophotometer (Hach Corporation, USA) equipped with a digestion system (DRB200) based on the principle of salicylic acid method. Then the degradation efficiency (DE) was calculated as Equation (1).

$$DE = \frac{C_0 - C_t}{C_0} \times 100\% \tag{1}$$

where, C_0 and C_t are the initial and final concentration of NH_4^+-N (mg/L), respectively.

The energy consumption (E, kW·h/g) during electrochemical process was calculated by Equation (2).

$$E = \frac{UIt}{(C_0 - C_t)V} \tag{2}$$

where, U is the cell potential (V), I is the current (A), t is the degradation time (s), V is the volume of solution (L).

The accelerated service lifetime tests were carried out by anodic polarization of the prepared electrodes at 100 mA/cm^2 in 0.5 mol/L H_2SO_4 solution at room temperature. The accelerated service lifetime of the electrode was defined as the duration from the initial value to the cell potential increasing to 5 V. The lifetime of electrode was calculated according to the empirical formula proposed by B. Correa-Lozano *et al.* shown as Equation (3) (Correa-Lozano *et al.* 1997).

$$\tau_1 = \left(\frac{i_2}{i_1}\right)^2 \tau_2 \tag{3}$$

where, τ_1 is the actual electrode lifetime, τ_2 is the accelerated lifetime, i_1 is the actual current density, i_2 is the accelerated current density.

RESULTS AND DISCUSSION

Surface properties of the electrodes

The surface morphology of the prepared electrodes was analyzed by SEM. As shown in Figure 1(a), the surface of Ti/MnO_x electrode was rough with large particles, suggesting the aggregation of MnO_x particles during preparation process. Ti/MnO_x-C electrode possessed smooth surface without obvious cracks (Figure 1(b)), indicating that the introduction of conductive carbon black could significantly affect the morphology and improve the surface integrity of the electrode. However, pinholes with size of ca. 20 nm were observed on the surface of electrode. Ti/Ce:MnO_x-C electrode displayed more dense and compact surface with smaller pinhole size (ca. 5 nm in Figure 1(c)). The surface evenness and compaction of electrode was important for electrochemical process, and might affect the lifetime of electrode (Santos *et al.* 2014). The SEM images suggested the significant improvement of surface evenness and compaction originated from carbon black and Ce addition.

Typical XRD patterns of Ti/MnO_x, Ti/MnO_x-C and Ti/Ce:MnO_x-C electrodes are shown in Figure S1 (Supporting Information). All of the diffraction peaks could be assigned to the hexagonal Ti (JCPDS No. 44-1294 and No. 89-3725) originating from Ti substrate without MnO_x phase observed, which might be caused by the amorphous MnO_x formed in

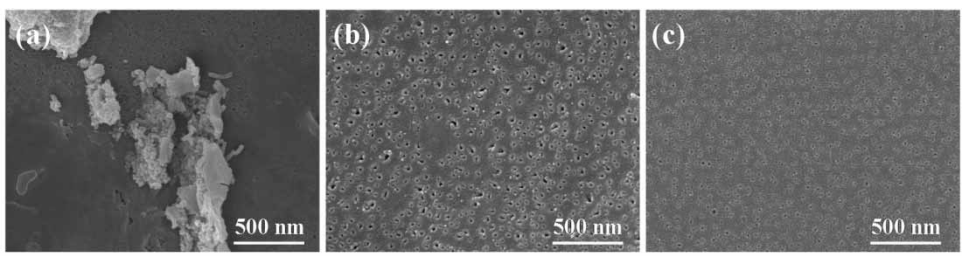

Figure 1 | SEM images of (a) Ti/MnO_x, (b) Ti/MnO_x-C, and (c) Ti/Ce:MnO_x-C electrodes.

the present conditions. Additionally, there was no diffraction peak of TiO_2 in the XRD patterns, which suggested that the Ti substrate was not oxidized during the preparation process. Therefore, the conductivity of Ti substrate was maintained to facilitate the electrochemical reaction.

XPS measurement was performed to investigate the chemical state of the electrode surface elements. The XPS survey spectra are presented in Figure S2, and the Mn and O photoelectron peaks are clearly observed. The fine structure of Mn 2p and O 1 s was investigated because the Mn oxidation state and oxygen species play important roles in the electrochemical processes. As shown in Figure 2, the Mn 2p peaks were fitted by considering two resolved doublets, Mn $2p_{1/2}$ and Mn $2p_{3/2}$, located at 653.9 eV and 642.2 eV, respectively. The coexistence of Mn(II), Mn(III) and Mn(IV) was evidenced by fitting the peaks, which could be assigned to MnO, Mn_2O_3 and MnO_2 as reported in the literature (Lee *et al.* 2011; Li *et al.* 2011; Wang *et al.* 2017a), even though there was no diffraction peak of manganese oxide found in the XRD results. The discrepancy might be caused by the poor crystallinity of manganese oxide formed in this study. The relative content of MnO_x phase calculated by Mn $2p_{3/2}$ is displayed in Table 1. It has been reported that MnO_2 was more beneficial for the electrochemical degradation of pollutants (Massa *et al.* 2018), and the results suggested that the introduction of Ce could enhance the Mn(IV) content while the addition of carbon black had little influence on the Mn oxidation state of Ti-based MnO_x electrode. The O 1s peak could be deconvoluted into the signal of lattice oxygen (O_L) and adsorbed oxygen (O_A). According to the peak fitting results shown in Table 1, the relative content of O_A, which has been reported as the most active oxygen and could play an important part in EO process, was similar for the three electrodes (Ramirez *et al.* 2014; Bian *et al.* 2019), suggesting the incorporation of carbon black and Ce had little effect on the relative O_A content of Ti-based MnO_x electrode.

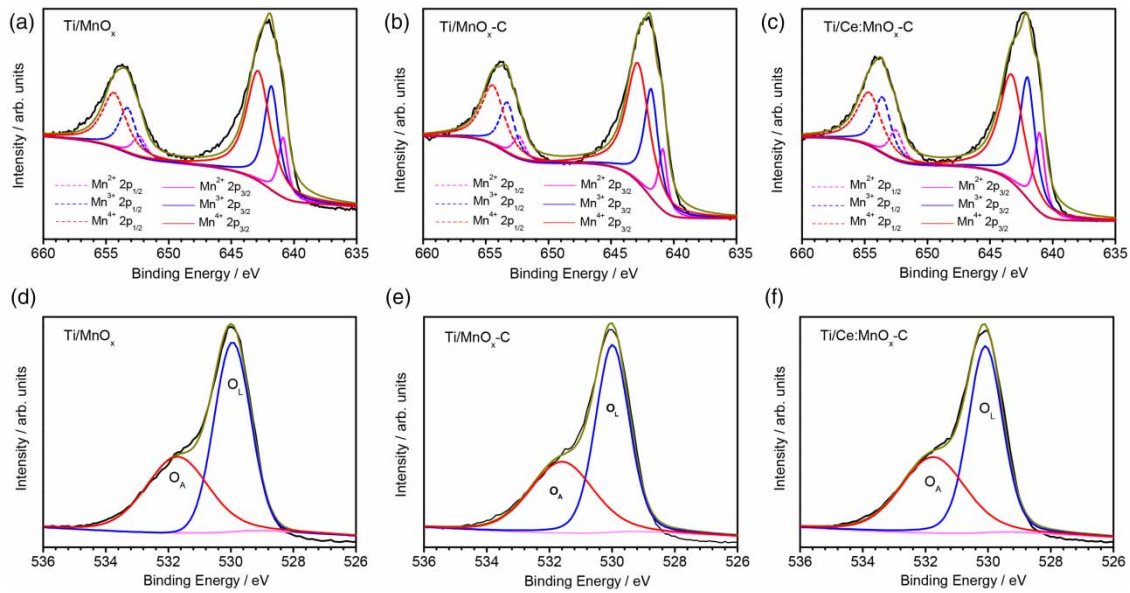

Figure 2 | The fine structure of (a, b, c) Mn 2p and (d, e, f) O 1s XPS spectra of (a, d) Ti/MnO_x, (b, e) Ti/MnO_x-C, and (c, f) Ti/Ce:MnO_x-C electrodes.

Table 1 | The characterization and electrochemical results of electrodes

	Relative content of Mn species (%)			Relative content of O species (%)					
Electrode	**Mn(II)**	**Mn(III)**	**Mn(IV)**	**O_L**	**O_A**	**R_s (Ω)**	**Cell potential (V)**	**Energy consumption (kW·h/g)**	**Electrode lifetime (h)**
Ti/MnO_x	12	32	56	57	43	654	5.2	0.28	2.2
Ti/MnO_x-C	11	32	57	58	42	80	4.6	0.24	7.5
Ti/Ce:MnO_x-C	8	26	66	57	43	9	3.4	0.18	54.6

Electrochemical characterization of the electrodes

The influence of additive on the electrochemical behavior of the Ti-based MnO_x electrode was investigated by voltammetry measurement. Typical CV curves of the Ti/MnO_x, Ti/MnO_x-C and Ti/Ce:MnO_x-C electrodes in 0.1 mol/L sodium sulfate solution are shown in Figure 3(a). There was no obvious redox signal observed except for the oxygen evolution, indicating that Ti-based MnO_x electrodes were electrochemically inactive in Na_2SO_4 solution (Duan *et al.* 2014). The electrochemical active surface area is related to the geometric area of the region enclosed by the CV curve, so the Ti/Ce:MnO_x-C electrode with larger electrochemical active surface area will present higher electrochemical activity in EO degradation of pollution. Additionally, the oxygen evolution current of Ti/Ce:MnO_x-C electrode was much higher than that of Ti/MnO_x and Ti/MnO_x-C at the same potential, which verified the superior electrochemical activity of Ti/Ce:MnO_x-C electrode (Duan *et al.* 2012). It has been reported that the NH_4^+-N degradation mechanism could be direct oxidation and indirect oxidation (Siddharth *et al.* 2018). In this work, NH_4^+-N was completely removed in the presence of Cl^- and the degradation efficiency was only 6.1% in the absence of Cl^- in the electrolyte (Figure S3). The electrochemical degradation results verified that NH_4^+-N was mainly degraded by indirect oxidation in this work. Ti-based MnO_x electrode showed enhanced performance for the electrochemical degradation of NH_4^+-N in the presence of Cl^- due to the generation of several chlorine-based oxidants, such as Cl_2, HOCl and ClO^- (Siddharth *et al.* 2018). As shown by the LSV profiles of electrodes in the presence of Cl^- (Figure 3(b)), the onset potential of Ti/Ce:MnO_x-C electrode was lower with higher current at the same potential, which indicated that Ce and C co-incorporation facilitated the electrochemical reaction of Ti-based MnO_x electrode.

In further investigation on the influence of additive on the electrochemical activity of Ti-based MnO_x electrode, EIS was used to determine the charge transfer resistance of electrodes. The Nyquist and equivalent circuit model for Ti/MnO_x, Ti/MnO_x-C and Ti/Ce:MnO_x-C electrodes are presented in Figure 4. In the equivalent circuit, the ohmic resistance and charge transfer resistance are presented as R_s and R_{ct}, respectively. According to the fitting results, the value of R_{ct} for Ti/MnO_x-C electrode was 80 Ω, which was significantly reduced compared with that for the Ti/MnO_x electrode (654 Ω), and the R_{ct} value was further reduced to 9 Ω for Ti/Ce:MnO_x-C electrode. The EIS measurement demonstrated that the Ce:MnO_x-C coating layer exhibited a much lower charge transfer resistance, which indicated the great improvement of electron transfer rate and conductivity of electrodes. The improvement of electron transfer rate was beneficial for the reduction of cell potential and energy consumption during the electrochemical process, which provided economic feasibility for electrochemical degradation of pollutants in wastewater (Hernández *et al.* 2016).

Electrochemical degradation of ammonia nitrogen

The catalytic performance of the Ti-based MnO_x electrodes for electrochemical degradation of NH_4^+-N (23 mg/L) was investigated in Na_2SO_4 (0.1 mol/L) solution with NaCl concentration of 400 mg/L, current density of 20 mA/cm^2 and pH of 9.0. Figure 5(a) illustrates the concentration of NH_4^+-N during the electrochemical degradation process with the prepared electrodes. The concentration of NH_4^+-N decreased gradually with the reaction proceed, and reached 0.2 mg/L at 90 min for Ti/MnO_x electrode. The degradation efficiency of Ti/MnO_x-C was comparable to that of Ti/Ce:MnO_x-C electrode. For

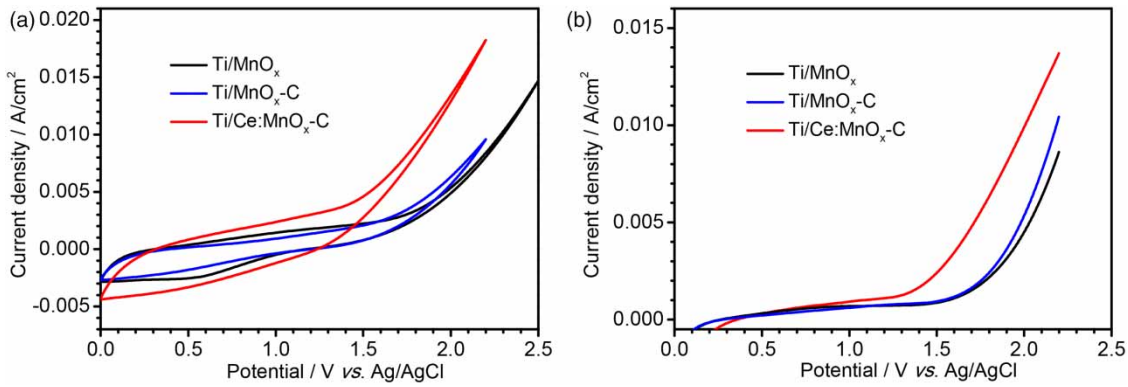

Figure 3 | (a) Cyclic voltammetry of Ti/MnO_x, Ti/MnO_x-C and Ti/Ce:MnO_x-C electrodes at a scan rate of 50 mV/s in a 0.1 mol/L Na_2SO_4 solution, and (b) linear sweep voltammetry of Ti/MnO_x, Ti/MnO_x-C and Ti/Ce:MnO_x-C electrodes at a scan rate of 10 mV/s in 0.1 mol/L Na_2SO_4 and 400 mg/L NaCl solution.

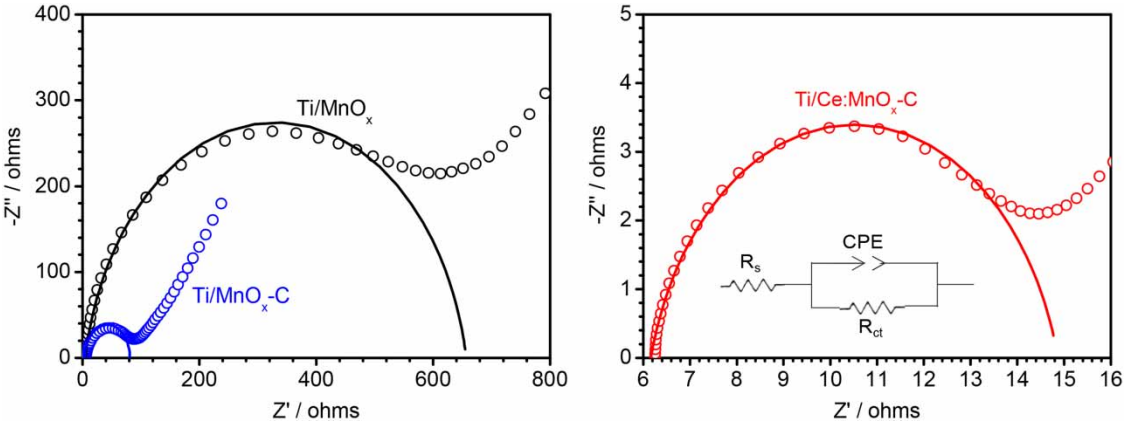

Figure 4 | Electrochemical impedance spectroscopy of Ti/MnO_x, Ti/MnO_x-C and Ti/Ce:MnO_x-C electrodes in 0.1 mol/L Na_2SO_4.

Ti/Ce:MnO_x-C electrode, the NH_4^+-N could be completely removed within 90 min, and the residual total nitrogen was 2.0 mg/L with nitrate of 5.1% (1.2 mg/L) and dichloramine of 3.4% (0.8 mg/L), which suggested that most of the ammonia nitrogen (91.5%) was mineralized to N_2. These results suggested that Ti-based MnO_x electrode was efficient for NH_4^+-N degradation. Figure 5(b) illustrates the corresponding cell potential during the electrochemical degradation process, which kept stable for each electrode. The cell potential of Ti/MnO_x-C electrode was lower than that of Ti/MnO_x. It is noteworthy that the cell potential of Ti/Ce:MnO_x-C electrode reduced by 35% compared to Ti/MnO_x, which was 3.4 V versus 5.2 V. The significant decrease of cell potential might be caused by the improved conductivity of electrode by co-incorporation of carbon black and Ce verified by the EIS results (Song *et al.* 2007; Wang *et al.* 2017b). The corresponding energy consumption during electrochemical process was calculated by Equation (2) and shown in Figure 5(c). The energy consumption increased as electrochemical degradation proceeded and reached 0.18 kW·h/g for Ti/Ce:MnO_x-C electrode when NH_4^+-N was totally degraded, which was reduced by 35% compared to the Ti/MnO_x electrode (0.28 kW·h/g). The cost of energy consumption is reduced to ca. US$ 20/kg (NH_4^+-N) for Ti/Ce:MnO_x-C electrode. These results indicated that the co-incorporation of carbon black and Ce could improve the conductivity of electrodes, leading to reduced cell potential and less energy consumption during electrochemical process (Jin *et al.* 2015).

The stability of electrode determines the electrode performance and commercial application, so in order to evaluate the stability of electrode, accelerated service life experiments were carried out in 0.5 mol/L sulfuric acid solution at 100 mA/cm^2. As displayed in Figure 6, the cell potential of Ti/MnO_x electrode increased significantly, suggesting the poor stability of Ti/MnO_x electrode, while the cell potential of Ti/Ce:MnO_x-C electrode was lower and much more stable than that of Ti/MnO_x. According to the empirical formula proposed by B. Correa-Lozano *et al.* (1997), the actual lifetime of Ti/Ce:MnO_x-C electrode was 54.6 h calculated by Equation (3), which was ca. 25 times that of Ti/MnO_x electrode (2.2 h). The improved stability of Ti/Ce:MnO_x-C electrode mainly originated from the co-incorporation of carbon black and Ce, which not only enhanced the conductivity but also improved the surface evenness of the electrode (Gargouri *et al.* 2014; Jin *et al.* 2015).

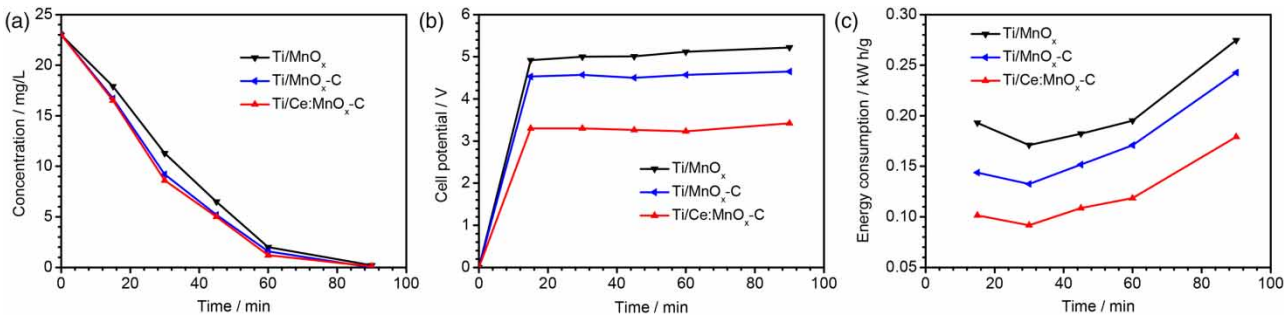

Figure 5 | (a) The concentration, (b) cell potential and (c) energy consumption of Ti/MnO_x, Ti/MnO_x-C and Ti/Ce:MnO_x-C electrodes during the degradation of ammonia nitrogen.

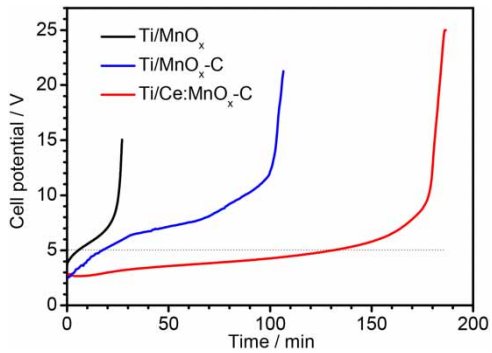

Figure 6 | Accelerated lifetime tests of Ti/MnO_x, Ti/MnO_x-C and Ti/Ce:MnO_x-C electrodes in 0.5 M H_2SO_4 solution at 100 mA/cm^2.

CONCLUSION

In summary, the Ti-based MnO_x electrode co-incorporated with carbon black and Ce was successfully prepared by spraying-calcination method. The surface properties, electrochemical performance, degradation activity and stability of Ti/Ce:MnO_x-C electrode were compared with those of the Ti/MnO_x electrode. The electrochemical results demonstrated that Ti/Ce:MnO_x-C electrode served as an efficient electrocatalyst to degrade NH_4^+-N completely with N_2 formation of 91.5%. The cell potential and energy consumption of Ti/Ce:MnO_x-C electrode were reduced by 35% and stability was improved by ca. 25 times. The superior performance of Ti/Ce:MnO_x-C electrode might benefit from its flat and integrated surface and low charge transfer resistance by co-incorporation of carbon black and Ce. This research provided a novel method for the modification of Ti-based MnO_x electrode, and would be helpful for the application of Ti-based MnO_x electrode in electrochemical degradation of NH_4^+-N and other organic pollutants.

ACKNOWLEDGEMENTS

This research was financially supported by National Natural Science Foundation of China (No. 21905035), LiaoNing Revitalization Talents Program (XLYC1907093), Guide Plan of Key Research and Development Program of Liaoning Province (2019JH8/10100096) and Fundamental Research Funds for the Central Universities (No. 3132019334), and the Initial Scientific Research Fund of Young Teachers in Shenyang University of Technology under Grant No. 200005782.

DATA AVAILABILITY STATEMENT

All relevant data are included in the paper or its Supplementary Information.

REFERENCES

Bacelo, H., Pintor, A. M. A., Santos, S. C. R., Boaventura, R. A. R. & Botelho, C. M. S. 2020 Performance and prospects of different adsorbents for phosphorus uptake and recovery from water. *Chem. Eng. J.* **381**, 122566.

Baddouh, A., El Ibrahimi, B., Rguitti, M. M., Mohamed, E., Hussain, S. & Bazzi, L. 2020 Electrochemical removal of methylene blue dye in aqueous solution using Ti/RuO_2-IrO_2 and SnO_2 electrodes. *Sep. Sci. Technol.* **55**, 1852–1861.

Bian, X., Xia, Y., Zhan, T., Wang, L., Zhou, W., Dai, Q. Z. & Chen, J. M. 2019 Electrochemical removal of amoxicillin using a Cu doped PbO_2 electrode: electrode characterization, operational parameters optimization and degradation mechanism. *Chemosphere* **233**, 762–770.

Brillas, E. & Martínez-Huitle, C. A. 2015 Decontamination of wastewaters containing synthetic organic dyes by electrochemical methods. An updated review. *Appl. Catal. B.* **166**, 603–643.

Choudhary, M., Kumar, R. & Neogi, S. 2020 Activated biochar derived from *Opuntia ficus-indica* for the efficient adsorption of malachite green dye, Cu^{+2} and Ni^{+2} from water. *J. Hazard. Mater.* **392**, 122441.

Correa-Lozano, B., Comninellis, C. & Battisti, A. D. 1997 Service life of Ti/SnO_2–Sb_2O_5 anodes. *J. Appl. Electrochem.* **27**, 970–974.

Del Moro, G., Prieto-Rodríguez, L., De Sanctis, M., Di Iaconi, C., Malato, S. & Mascolo, G. 2016 Landfill leachate treatment: comparison of standalone electrochemical degradation and combined with a novel biofilter. *Chem. Eng. J.* **288**, 87–98.

Dominguez, C. M., Oturan, N., Romero, A., Santos, A. & Oturan, M. A. 2018 Removal of lindane wastes by advanced electrochemical oxidation. *Chemosphere* **202**, 400–409.

Duan, X., Ma, F., Yuan, Z., Chang, L. & Jin, X. 2012 Comparative studies on the electro-catalytic oxidation performance of surfactant-carbon nanotube-modified PbO_2 electrodes. *J. Electroanal. Chem.* **677**, 90–100.

Duan, X., Zhao, Y., Liu, W., Chang, L. & Li, X. 2014 Electrochemical degradation of p-nitrophenol on carbon nanotube and Ce-modified-PbO_2 electrode. *J. Taiwan Inst. Chem. E* **45**, 2975–2985.

Garcia-Segura, S., Ocon, J. D. & Chong, M. N. 2018 Electrochemical oxidation remediation of real wastewater effluents-A review. *Process Saf. Environ. Prot.* **113**, 48–67.

Gargouri, B., Gargouri, O. D., Gargouri, B., Trabelsi, S. K., Abdelhedi, R. & Bouaziz, M. 2014 Application of electrochemical technology for removing petroleum hydrocarbons from produced water using lead dioxide and boron-doped diamond electrodes. *Chemosphere* **117**, 309–315.

Gopalakrishnan, G., Somanathan, A. & Jeyakumar, R. B. 2019 Combination of solar advanced oxidation processes and biological treatment strategy for the decolourization and degradation of pulp and paper mill wastewater. *Desalin. Water Treat.* **158**, 87–96.

Hernández, S., Ottone, C., Varetti, S., Fontana, M., Pugliese, D., Saracco, G., Bonelli, B. & Armandi, M. 2016 Spin-coated vs. electrodeposited Mn oxide films as water oxidation catalysts. *Materials* **9**, 296.

Hui, H., Wang, H., Mo, Y., Yin, Z. & Li, J. X. 2019 Optimal design and evaluation of electrocatalytic reactors with nano-MnO_x/Ti membrane electrode for wastewater treatment. *Chem. Eng. J.* **376**, 120190.

Imran, M., Iqbal, M. M., Iqbal, J., Shah, N. S., Khan, Z. U., Murtaza, B., Amjad, M., Ali, S. & Rizwan, M. 2021 Synthesis, characterization and application of novel MnO and CuO impregnated biochar composites to sequester arsenic (As) from water: modeling, thermodynamics and reusability. *J. Hazard. Mater.* **401**, 12338.

Jiang, J. & Kucernak, A. 2002 Electrochemical supercapacitor material based on manganese oxide: preparation and characterization. *Electrochim. Acta* **47**, 2381–2386.

Jin, Y., Wang, F., Xu, M., Hun, Y., Fang, W., Wei, Y. & Zhu, C. 2015 Preparation and characterization of Ce and PVP co-doped PbO_2 electrode for waste water treatment. *J. Taiwan Inst. Chem. E* **51**, 135–142.

Kaur, P., Kushwaha, J. P. & Sangal, V. K. 2017 Evaluation and disposability study of actual textile wastewater treatment by electro-oxidation method using Ti/RuO_2 anode. *Process Saf. Environ. Prot.* **111**, 13–22.

Lee, J., Park, G. S., Lee, H. I., Kim, S. T., Cao, R. G., Liu, M. L. & Cho, J. 2011 Ketjenblack carbon supported amorphous manganese oxides nanowires as highly efficient electrocatalyst for oxygen reduction reaction in alkaline solutions. *Nano Lett.* **11**, 5362–5366.

Li, Q., Liu, J., Zou, J., Chunder, A., Chen, Y. & Zhai, L. 2011 Synthesis and electrochemical performance of multi-walled carbon nanotube/polyaniline/MnO_2 ternary coaxial nanostructures for supercapacitors. *J. Power Sources* **196**, 565–572.

Li, X., Xu, H. & Yan, W. 2016 Fabrication and characterization of PbO_2 electrode modified withpolyvinylidene fluoride (PVDF). *Appl. Surf. Sci.* **389**, 278–286.

Liu, Z. Q., Huang, C. X., Li, J. Y., Yang, J. J., Qu, B., Yang, S. Q., Cui, Y. H., Yan, Y. H., Sun, S. Q. & Wu, X. H. 2021 Activated carbon catalytic ozonation of reverse osmosis concentrate after coagulation pretreatment from coal gasification wastewater reclamation for zero liquid discharge. *J. Clean. Prod.* **286**, 124951.

Mamelkina, M. A., Herraiz-Carbone, M., Cotillas, S., Lacasa, E., Saez, C., Tuunila, R., Sillanpaa, M., Hakkinen, A. & Rodrigo, M. A. 2020 Treatment of mining wastewater polluted with cyanide by coagulation processes: a mechanistic study. *Sep. Purif. Technol.* **237**, 116345.

Martínez-Huitle, C. A., De Battisti, A., Ferro, S., Reyna, S., Cerro-Lopez, M. & Quiro, M. A. 2008 Removal of the pesticide methamidophos from aqueous solutions by electrooxidation using Pb/PbO_2, Ti/SnO_2, and Si/BDD electrodes. *Environ. Sci. Technol.* **42**, 6929–6935.

Massa, A., Hernández, S., Ansaloni, S., Castellino, M., Russo, N. & Fino, D. 2018 Enhanced electrochemical oxidation of phenol over manganese oxides under mild wet air oxidation conditions. *Electrochim. Acta* **273**, 53–62.

Polcaro, A. M., Palmas, S., Renoldi, F. & Mascia, M. 1999 On the performance of Ti/SnO_2 and Ti/PbO_2 anodes in electrochemical degradation of 2-chlorophenol for wastewater treatment. *J. Appl. Electrochem.* **29**, 147–151.

Ramirez, A., Hillebrand, P., Stellmach, D., May, M. M., Bogdanoff, P. & Fiechter, S. 2014 Evaluation of MnO_x, Mn_2O_3, and Mn_3O_4 electrodeposited films for the oxygen evolution reaction of water. *J. Phys. Chem. C* **118**, 14073–14081.

Santos, D., Lopes, A., Pacheco, M. J., Gomes, A. & Ciriaco, L. 2014 The oxygen evolution reaction at Sn-Sb oxide anodes: influence of the oxide preparation mode. *J. Electrochem. Soc.* **161**, H564–H572.

Siddharth, K., Chan, Y., Wang, L. & Shao, M. 2018 Ammonia electro-oxidation reaction: recent development in mechanistic understanding and electrocatalyst design. *Electrocatalysis* **9**, 151–157.

Silva, D. B., Cruz-Alcalde, A., Sans, C., Gimenez, J. & Esplugas, S. 2019 Performance and kinetic modelling of photolytic and photocatalytic ozonation for enhanced micropollutants removal in municipal wastewaters. *Appl. Catal. B.* **249**, 211–217.

Song, Y., Wei, G. & Xiong, R. 2007 Structure and properties of PbO_2-CeO_2 anodes on stainless steel. *Electrochim. Acta* **52**, 7022–7027.

Tavangar, T., Karimi, M., Rezakazemi, M., Reddy, K. R. & Aminabhavi, T. M. 2020 Textile waste, dyes/inorganic salts separation of cerium oxide-loaded loose nanofiltration polyethersulfone membranes. *Chem. Eng. J.* **385**, 123787.

Tavares, M. G., da Silva, L. V. A., Solano, A. M. S., Tonholo, J., Martinez-Huitle, C. A. & Zanta, C. L. P. S. 2012 Electrochemical oxidation of Methyl Red using Ti/$Ru_{0.3}Ti_{0.7}O_2$ and Ti/Pt anodes. *Chem. Eng. J.* **204**, 141–150.

Wang, Y., Cui, J., Luo, L., Zhang, J., Wang, Y., Qin, Y., Zhang, Y., Shu, X., Lv, J. & Wu, Y. 2017a One-pot synthesis of NiO/Mn_2O_3 nanoflake arrays and their application in electrochemical biosensing. *Appl. Surf. Sci.* **423**, 1182–1187.

Wang, Z., Xu, M., Wang, F., Liang, X., Wei, Y., Hu, Y., Zhu, C. & Fang, W. 2017b Preparation and characterization of a novel Ce doped PbO_2 electrode based on NiO modified Ti/TiO_2NTs substrate for the electrocatalytic degradation of phenol wastewater. *Electrochim. Acta* **247**, 535–547.

Wang, J. C., Cui, C. X., Kong, Q. Q., Ren, C. Y., Li, Z. J., Qu, L. B., Zhang, Y. P. & Jiang, K. 2018 Mn-Doped g-C_3N_4 nanoribbon for efficient visible-light photocatalytic water splitting coupling with methylene blue degradation. *ACS Sustain. Chem. Eng.* **6**, 8754–8761.

Wiechen, M., Zaharieva, I., Dau, H. & Kurz, P. 2012 Layered manganese oxides for water-oxidation: alkaline earth cations influence catalytic activity in a photosystem II-like fashion. *Chem. Sci.* **3**, 2330–2339.

Wu, Z. Y., Zhu, W. P., Liu, Y., Zhou, L. L., Liu, P. X. & Xu, J. 2021 An integrated biological-electrocatalytic process for highly-efficient treatment of coking wastewater. *Bioresour. Technol.* **339**, 125584.

Xiang, X., Xia, F., Zhan, L. & Xie, B. 2015 Preparation of zinc nano structured particles from spent zinc manganese batteries by vacuum separation and inert gas condensation. *Sep. Purif. Technol.* **142**, 227–233.

Xu, X., Zhao, J., Bai, S., Mo, R., Yang, Y., Liu, W., Tang, X., Yu, H. & Zhu, Y. 2019 Preparation of novel Ti-based MnO_x electrodes by spraying method for electrochemical oxidation of Acid Red B. *Water Sci. Technol.* **80**, 365–376.

Yang, S., Liang, X., Zhang, D., Lin, C. H., Zhao, J. Q., Zhu, Y. P., Chen, Z. S., Wang, H., Wang, H. & Li, J. X. 2018 MnO_x/Ti composite membrane anode in the electrocatalytic membrane reactor for phenolic wastewater treatment. *J. Electrochem. Soc.* **165**, E20–E27.

Yue, H., Xue, L. & Chen, F. 2017 Efficiently electrochemical removal of nitrite contamination with stable RuO_2-TiO_2/Ti electrodes. *Appl. Catal. B: Environ.* **206**, 683–691.

Zhu, K., Wang, X., Ma, X., Sun, Z. R. & Hu, X. 2019 Comparative degradation of atrazine by anodic oxidation at graphite and platinum electrodes and insights into electrochemical behavior of graphite anode. *Electrocatalysis* **10**, 35–44.

Zöllig, H., Morgenroth, E. & Udert, K. M. 2015 Inhibition of direct electrolytic ammonia oxidation due to a change in local pH. *Electrochim. Acta* **165**, 348–355.

First received 13 July 2021; accepted in revised form 12 September 2021. Available online 27 September 2021